IEEE Access
Multidisciplinary ⋮ Rapid Review ⋮ Open Access Journal

Received 13 March 2023, accepted 21 March 2023, date of publication 28 March 2023, date of current version 3 April 2023.

Digital Object Identifier 10.1109/ACCESS.2023.3262515

RESEARCH ARTICLE

Design of Zero-Differential Steering Controller for Tracked Vehicles With Hydraulic-Mechanical Transmission Based on Particle Swarm Optimization Algorithm

WEIJIAN JIA[1], (Student Member, IEEE), XIXIA LIU[1], (Member, IEEE), CHUANQING ZHANG[1], (Member, IEEE), MIANHAO QIU[1], (Member, IEEE), YONGYING TAN[2], (Member, IEEE), AND ZHANG YU[1], (Member, IEEE)

[1]Army Academy of Armored Forces, Beijing 100072, China
[2]Beijing Special Engineering and Design Institute, Beijing 100028, China

Corresponding author: Xixia Liu (1244006991@qq.com)

This work was supported by the National Key Research and Development Program of China under Grant 2018YFC0810500.

ABSTRACT The handling stability of tracked vehicles not only affects the handling convenience of drivers but is also an important part of vehicle active safety. A zero-differential steering controller for tracked vehicles with hydraulic-mechanical transmissions was designed in this paper. First, the working principle of the steer-by-wire systems of tracked vehicles was analyzed, and the vehicle speed calculation model was established. Then, the steering dynamics model of the tracked vehicle was established based on the shear stress model. Finally, based on the particle swarm optimization algorithm, the established tracked vehicle steering dynamics model was iteratively solved, and the optimal yaw rate gain K_r was calculated in real time and used for vehicle steering control. The steering control simulation model of tracked vehicles was established in MATLAB/Simulink, and the control effect of the designed steering controller was verified by the simulation. The control effect was evaluated by the comprehensive evaluation index of the handling stability. The simulation results showed that the steering controller based on the particle swarm optimization algorithm effectively improved the handling stability of the tracked vehicle and reduced the burden on the driver.

INDEX TERMS Particle swarm optimization algorithm, steer-by-wire system, tracked vehicle, zero-differential steering controller.

I. INTRODUCTION

The steering system is an important component of vehicles, and its characteristics play a decisive role in vehicle handling stability and safety [1]. The steering wheel of the conventional steering system is mechanically connected to the steering mechanism, and the steering ratio is fixed. With change in vehicle speed and lateral acceleration, vehicle steering characteristics show strong nonlinear time-varying characteristics [2], [3], [4]. In order to control the vehicle to travel along the reference trajectory, the driver must always predict and adjust the steering behavior based on the change in vehicle steering characteristics [5]. This design of a fixed steering ratio makes it difficult for vehicles to meet the requirements for handling stability at high speeds, and it can also easily to cause driver fatigue [6]. A steer-by-wire (SBW) system eliminates the mechanical connection between the steering wheel and the steering mechanism. Steer-by-wire technology is used to control the steering of a vehicle through electrical signals [7], [8]. The steering ratio can be arbitrarily designed, so that the vehicle handling stability and safety are significantly improved [9]. The research on improving the

The associate editor coordinating the review of this manuscript and approving it for publication was Giulio Reina.

handling stability and safety of SBW systems was mainly for wheeled vehicles, and less research has been conducted on the handling stability and safety of SBW systems for tracked vehicles. The working environment of tracked vehicles is complex, and the driving principle is different from that of wheeled vehicles [10], [11], [12]. With the development of high-speed tracked vehicles, the research on the handling stability of SBW systems under the high-speed steering of tracked vehicles has attracted widespread attention.

Researchers have conducted in-depth research on how to improve the handling stability and comfort of the SBW system. Chai et al. [13] evaluated the driving characteristics of drivers in different age groups and determined that older drivers have driving characteristics with large reaction and maneuvering delays. By adjusting the steering gain and steering derivative time constant of the SBW control model, the driving comfort of an elderly driver was effectively improved. Li et al. [14] analyzed the influence of the steering ratio on the steering sensitivity and expected yaw rate gain through simulations. Through the analysis, it was found that the fixed steering ratio method of a vehicle at high speeds might cause the vehicle to oversteer and the vehicle handling stability to decrease. To improve the vehicle handling stability, it was necessary to increase the steering ratio at high speeds. Oh et al [15]. used the front wheel angle and vehicle speed as control inputs to establish the vehicle understeer gradient equation and performed feedforward control on the steering ratio. This method increased the steering ratio of the vehicle at high speeds and improved the vehicle handling stability. Based on the work of Oh et al., Fahami et al. [16] further considered the influence of the initial front wheel angle and improved the understeer gradient equation. The simulation results showed that this method allowed the vehicle to achieve variable steering ratio control in the steering process and improved the vehicle maneuverability and handling stability. Zheng et al. [17] proposed a steering control strategy with a variable steering ratio by setting a fixed yaw rate gain. Then, a vehicle steering dynamics model was established using the genetic algorithm to solve the optimal yaw rate gain in real time. The experimental results showed that using the optimized yaw rate gain to design the SBW steering ratio could effectively improve the vehicle handling stability and reduce the driving burden. Krishna et al. [18] took the yaw rate error, the steering angle given by the driver, and the vehicle body side slip angle as control inputs, and they proposed a fuzzy-logic-based yaw stability controller for the active front steering of a four-wheeled road vehicle by using a steer-by-wire system. After improving the steering stability of the vehicle by setting a fixed yaw rate gain, Dongzr et al. [19] further proposed a rear-wheel active steering control strategy based on the linear-quadratic regulator (LQR) algorithm to improve the trajectory tracking accuracy of the vehicle. Jin et al. [20] established a vehicle steering dynamics model, proposed a comprehensive evaluation index for vehicle steering control that integrated yaw, lateral, and roll motions, optimized the steering ratio of the vehicle under different working conditions by the genetic algorithm, and proposed a corresponding anti-rollover control strategy for vehicle rollover. The simulation results showed that the proposed method improved the low-speed steering flexibility and high-speed steering stability, and it effectively reduced the risk of vehicle rollover in some conditions.

In this paper, a tracked vehicle with a hydraulic-mechanical transmission was taken as the research object, and a zero-differential steering controller was designed for the SBW system. The working principle of the SBW system was analyzed, and the vehicle speed calculation model was established. Based on the shear stress model, the steering dynamics model of a tracked vehicle was established, and the relationship between the yaw rate $\dot{\theta}$ and the circumferential velocity difference of the sprocket Δu was calculated when the tracked vehicle steered on a sand road at different theoretical centroid speeds v_{th}. The yaw rate gain K_r was selected as the control object, and the steering controller was designed based on the particle swarm optimization (PSO) algorithm. The optimal K_r was obtained in real time and used for the tracked vehicle steering control. The steering control simulation model of the tracked vehicle was established by using MATLAB/Simulink, and the effectiveness of the designed SBW controller of the tracked vehicle was simulated and verified.

II. PRINCIPLE OF ZERO-DIFFERENTIAL STEERING CONTROL

A. WORKING PRINCIPLE OF STEER-BY-WIRE (SBW) SYSTEM

The structure of the tracked vehicle SBW system is shown in Fig. 1. n_e is the engine speed (r/min). i_q is the ratio from the engine to the fixed-shaft gearbox. i_{bn} is the ratio of the fixed-shaft gearbox when the vehicle is driving in n-th gear. i_p is the ratio of the engine to the variable pump. i_{yl} and i_{yr} are the ratios of the left and right hydraulic pump-motor systems, respectively, where $i_{yl} = 1/\varepsilon_p\eta$ and $i_{yr} = -1/\varepsilon_p\eta$. ε_p is the variable pump displacement ratio. η is the transfer efficiency of the hydraulic pump-motor system. i_M is the ratio of the hydraulic motor to the sun gear of the planetary gear. k is the

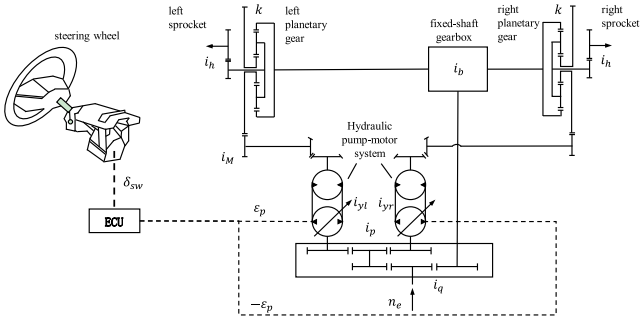

FIGURE 1. Steer-by-wire (SBW) system structure of the tracked vehicle.

characteristic parameter of the planetary gear. i_h is the ratio of the side reducer.

The steering wheel angle sensor collects the steering wheel angle signal δ_{sw} and sends it to the electronic control unit (ECU). According to the steering control rules, the ECU converts δ_{sw} into command variable pump displacements ε_p and $-\varepsilon_p$ to the left and right hydraulic pump-motor systems, respectively, and changes the transmission ratios i_{yl} and i_{yr} of the hydraulic pump-motor system on both sides. The hydraulic motors on the left and right sides have the same speed and the opposite rotation directions. Through the transmission mechanism, the sun gears on both sides of the planetary gear rotate in the opposite direction at the same speed, resulting in an increase in the speed of the sprocket on one side and a decrease in the speed of the sprocket on the other side.

The traditional steering system control rules usually set the corresponding relationship i_ε between the steering wheel angle and the displacement ratio of the variable pump as a fixed value:

$$i_\varepsilon = \frac{\delta_{sw}}{\varepsilon_p}. \tag{1}$$

The control principle of this method is simple, but it is difficult to adapt to the nonlinear characteristics of tracked vehicles during high-speed steering [21]. The design of vehicle SBW control rules by changing the yaw rate gain can effectively reduce the driver's driving burden. The yaw rate gain K_r of the tracked vehicle is the ratio of the yaw rate $\dot{\theta}$ to δ_{sw}, which can be expressed as follows:

$$K_r = \frac{\dot{\theta}}{\delta_{sw}}. \tag{2}$$

$\dot{\theta}$ is determined by the theoretical centroid speed v_{th} of the tracked vehicle and the circumferential velocity difference of the sprocket Δu. It can be expressed as follows:

$$\dot{\theta} = G_{\dot{\theta}}^{\Delta u} \Delta u. \tag{3}$$

where $G_{\dot{\theta}}^{\Delta u}$ is the corresponding relationship between $\dot{\theta}$ and Δu when the tracked vehicle turns at different v_{th} values. For a zero-differential steering tracked vehicle, the theoretical centroid speed v_{th} is determined by the circumferential velocity of the sprocket on both sides, $v_{th} = (u_l + u_r)/2$, and u_l and u_r are the circumferential velocities of the sprocket on both sides.

B. VEHICLE SPEED CALCULATION MODEL

A part of the engine power is transmitted to the fixed-shaft gearbox for straight-line driving and speed changes of the tracked vehicle, and the other part is transmitted to the hydraulic pump-motor steering system for the vehicle steering. When the vehicle is driving straight, the transmission ratio i_s from the engine to the sprocket can be expressed as follows:

$$i_s = \frac{(1+k)\, i_q i_{bn}}{k i_h}. \tag{4}$$

When the tracked vehicle turns, the ratios i_{tl} and i_{tr} of the engine to the left and right sprockets change, as follows:

$$i_{tl} = \frac{(1+k)\, i_q i_{bn} i_p i_{yl} i_M}{i_q i_{bn} + k i_p i_{yl} i_M}, \tag{5}$$

$$i_{tr} = \frac{(1+k)\, i_q i_{bn} i_p i_{yr} i_M}{i_q i_{bn} + k i_p i_{yr} i_M}. \tag{6}$$

u_l and u_r can be expressed as follows:

$$u_l = \frac{\pi n_e r \left(i_q i_{bn} + k i_p i_{yl} i_M\right)}{30\,(1+k)\, i_q i_{bn} i_p i_{yl} i_M i_h}, \tag{7}$$

$$u_r = \frac{\pi n_e r \left(i_q i_{bn} + k i_p i_{yr} i_M\right)}{30\,(1+k)\, i_q i_{bn} i_p i_{yr} i_M i_h}, \tag{8}$$

where r is the radius of the sprocket.

When the tracked vehicle is driving at v_{th}, the variable pump displacement ε_p is determined by Δu, and it can be expressed as follows:

$$\varepsilon_p = \frac{15 \Delta u\,(1+k)\, i_p i_M i_h}{n_e \pi r \eta} \tag{9}$$

The yaw rate $\dot{\theta}$ obtained by the Formulas (3) and (9) can be expressed as follows:

$$\dot{\theta} = \frac{G_{\dot{\theta}}^{\Delta u} \varepsilon_p n_e \pi r \eta}{15\,(1+k)\, i_p i_M i_h}. \tag{10}$$

The i_ε of the SBW system is determined by the yaw rate gain K_r, and it can be expressed as follows:

$$i_\varepsilon = \frac{\delta_{sw}}{\varepsilon_p} = \frac{n_e \pi r \eta G_{\dot{\theta}}^{\Delta u}}{15\,(1+k)\, i_p i_M i_h K_r}. \tag{11}$$

III. STEERING DYNAMICS MODEL

The following assumptions were made in the process of establishing the tracked vehicle steering dynamics model:

(1) The centroid position of the tracked vehicle is located in the geometric center of the vehicle.

(2) Track subsidence and side pushing effects of the track slab are neglected.

(3) The track is not stretchable, and the ground pressure at each point on the track ground plane is evenly distributed when the vehicle is stationary. Thus, ignoring the influence of the track width on the ground pressure is neglected.

(4) During the steering process of the tracked vehicle, the force on the track is calculated by the following shear stress model [22]:

$$\tau = (c + \sigma \tan\phi)\left(1 - e^{-j/K}\right) \tag{12}$$

where, τ is the shear stress at any point on the track, c is the soil cohesion, σ is the normal stress, ϕ is the angle of internal shearing resistance of the terrain, j is the shear displacement, and K is the shear deformation modulus.

A. KINEMATICS MODEL OF TRACKED VEHICLE

In order to facilitate the analysis, the geodetic coordinate system XOY was established, and the body coordinate system xoy was established at the centroid of the tracked vehicle. The coordinate origin o coincides with the centroid position, and the x-axis direction is the forward direction of the tracked vehicle. The relationship between the motion parameters of the tracked vehicle is shown in Fig. 2. v is the actual centroid velocity of the tracked vehicle under the geodetic coordinate system XOY. v_x and v_y are the components of v in the x-direction and y-direction, respectively, and $v = \sqrt{v_x^2 + v_y^2}$. θ is the yaw angle of the tracked vehicle. φ is the angle between v and the X-axis. β is the sideslip angle, and $\beta = \arctan\left(v_y/v_x\right)$. L is the length of the track contact with the ground. B is the distance between the track center lines on both sides. b is the width of the unilateral track. ψ is the angle between the direction of the velocity at a point on the track and the x-axis. O_l and O_r are the instantaneous steering centers of left-side track and right-side track respectively. d is the offset of the steering center O_c relative to the y-axis, $d = v_y/\dot{\theta}$.

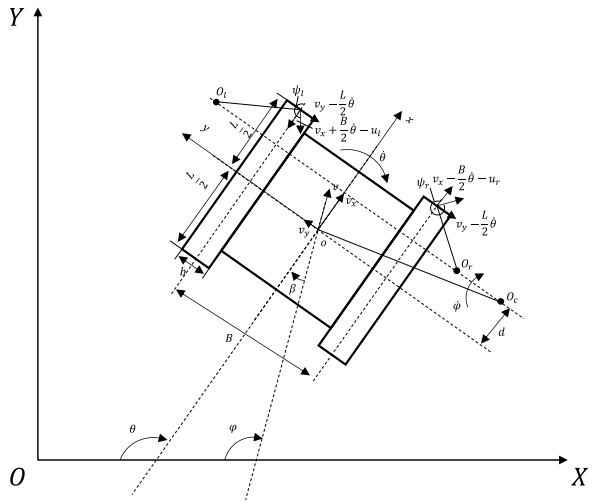

FIGURE 2. Relationship between the motion parameters of the tracked vehicle during steering.

The trajectory of the tracked vehicle when turning under XOY can be expressed as follows:

$$\begin{cases} X = \int_0^t v\cos(\theta - \beta)\mathrm{d}t \\ Y = \int_0^t v\sin(\theta - \beta)\mathrm{d}t \end{cases} \tag{13}$$

The accelerations a_x and a_y of the vehicle centroid along the x-axis and y-axis can be expressed as follows:

$$\begin{cases} a_x = \dot{v}_x + v_y\dot{\theta} \\ a_y = \dot{v}_y - v_x\dot{\theta} \end{cases} \tag{14}$$

In the geodetic coordinate system XOY, each point on the same track center line has the same velocity in the x-direction. The speed of a point (x_p, y_p) on the left track center line in the y-direction is determined by $\dot{\theta}$ and the x-coordinate value x_p of the point. The shear velocities v_{sxl} and v_{sxr} in the x-direction and the shear velocities v_{syl} and v_{syr} in the y-direction of this point and the symmetric point $(x_p, -y_p)$ on the right track with respect to the x-axis can be expressed as follows:

$$\begin{cases} v_{sxl} = v_x + \dfrac{B}{2}\dot{\theta} - u_l \\ v_{sxr} = v_x - \dfrac{B}{2}\dot{\theta} - u_r \\ v_{syl} = v_{syr} = v_y - x_p\dot{\theta}. \end{cases} \tag{15}$$

The angle between the speed of a point on the center line of the track on both sides and the x-axis can be expressed as follows:

$$\begin{cases} \psi_l = \arccos\left(v_{sxl}/\sqrt{v_{sxl}^2 + v_{syl}^2}\right) \\ \psi_r = \arccos\left(v_{sxr}/\sqrt{v_{sxr}^2 + v_{syr}^2}\right). \end{cases} \tag{16}$$

The slip ratios δ_l and δ_r of the left and right tracks, respectively, can be expressed as follows:

$$\begin{cases} \delta_l = \dfrac{v_{sxl}}{\max\left(u_l + v_{sxl}, u_l\right)} \\ \delta_r = \dfrac{v_{sxr}}{\max\left(u_r + v_{sxr}, u_r\right)}. \end{cases} \tag{17}$$

During the steering process of the tracked vehicle, the shear displacements j_l and j_r of a point (x_p, y_p) on the center line of the left track and the symmetric point $(x_p, -y_p)$ on the right track can be obtained by integrating the shear velocity, and they can be expressed as follows:

$$\begin{cases} j_{xl} = \int_0^t v_{sxl}\mathrm{d}t = \left(\dfrac{v_{sxl}}{u_l}\right)\left(\dfrac{L}{2} - x_p\right) \\ j_{xr} = \int_0^t v_{sxr}\mathrm{d}t = \left(\dfrac{v_{sxr}}{u_r}\right)\left(\dfrac{L}{2} - x_p\right), \end{cases} \tag{18}$$

$$\begin{cases} j_{yl} = \dfrac{1}{u_l}\left(v_y - \dfrac{L}{2}\dot{\theta}\right)\left(\dfrac{L}{2} - x_p\right) + \dfrac{1}{2u_l}\dot{\theta}\left(\dfrac{L}{2} - x_p\right)^2 \\ j_{yr} = \dfrac{1}{u_r}\left(v_y - \dfrac{L}{2}\dot{\theta}\right)\left(\dfrac{L}{2} - x_p\right) + \dfrac{1}{2u_r}\dot{\theta}\left(\dfrac{L}{2} - x_p\right)^2, \end{cases} \tag{19}$$

$$\begin{cases} j_l = \sqrt{j_{xl}^2 + j_{yl}^2} \\ j_r = \sqrt{j_{xr}^2 + j_{yr}^2}. \end{cases} \tag{20}$$

B. STEERING FORCE ANALYSIS

The inertial force generated by the steering of the tracked vehicle causes changes of the track ground pressures on both sides. The normal load distribution of the track on both sides under the influence of the inertial force is shown in Fig. 3.

The components ma_x and ma_y of the inertial force in the x-direction and y-direction, respectively, redistribute the ground pressure on the unilateral track. The unit area ground pressures p_l and p_r at a point on the left track (x_p, y_p) and the symmetric point on the right track $(x_p, -y_p)$ can be expressed

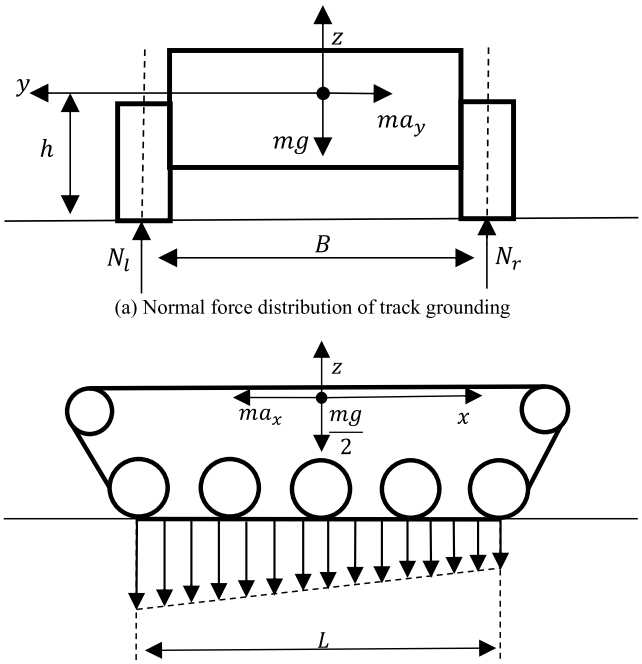

(a) Normal force distribution of track grounding

(b) Ground pressure distribution of road wheels on unilateral track

FIGURE 3. Normal load distribution of the track on both sides under influence of inertial forces.

as follows:

$$\begin{cases} p_l = \dfrac{mg}{2bL} - \dfrac{ma_y h}{BbL} - \dfrac{6ma_x hx_p}{bL^3} \\ p_r = \dfrac{mg}{2bL} + \dfrac{ma_y h}{BbL} - \dfrac{6ma_x hx_p}{bL^3}, \end{cases} \tag{21}$$

where h is the height of the centroid of the tracked vehicle.

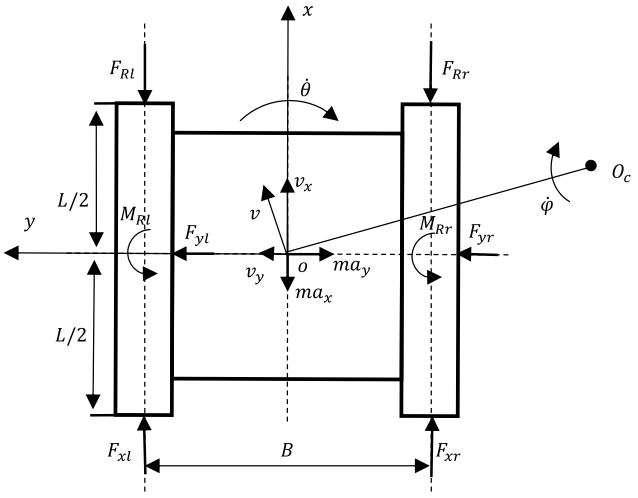

FIGURE 4. Steering forces of the tracked vehicle.

The forces on the track when the tracked vehicle turns are shown in Fig. 4. F_{xl} and F_{xr} are the components of the shear force of the left and right tracks and the ground in the x-direction, respectively. F_{yl} and F_{yr} are the components of the shear force in the y-direction, respectively. M_{Rl} and M_{Rr} are the steering resistance torques of the track on both sides, and F_{Rl} and F_{Rr} are the rolling resistances of the track on both sides. By Formulas (12) and (16)-(21), the shear force of the track on both sides in the x-direction and y-direction can be obtained, which can be expressed as follows:

$$\begin{cases} F_{xl} = \int_{-\frac{L}{2}}^{\frac{L}{2}} (c + p_l \tan\phi)\left(1 - e^{-\frac{j_l}{K}}\right) b\cos(\psi_l + \pi)\,\mathrm{d}x \\ F_{xr} = \int_{-\frac{L}{2}}^{\frac{L}{2}} (c + p_r \tan\phi)\left(1 - e^{-\frac{j_r}{K}}\right) b\cos(\psi_l + \pi)\,\mathrm{d}x, \end{cases} \tag{22}$$

$$\begin{cases} F_{yl} = \int_{-\frac{L}{2}}^{\frac{L}{2}} (c + p_l \tan\phi)\left(1 - e^{-\frac{j_l}{K}}\right) b\sin(\psi_l + \pi)\,\mathrm{d}x \\ F_{yr} = \int_{-\frac{L}{2}}^{\frac{L}{2}} (c + p_r \tan\phi)\left(1 - e^{-\frac{j_r}{K}}\right) b\sin(\psi_l + \pi)\,\mathrm{d}x. \end{cases} \tag{23}$$

The rolling resistances F_{Rl} and F_{Rr} on both sides of the track can be expressed as follows:

$$\begin{cases} F_{Rl} = f\left(\dfrac{mg}{2} - \dfrac{ma_y h}{B}\right) \\ F_{Rr} = f\left(\dfrac{mg}{2} + \dfrac{ma_y h}{B}\right), \end{cases} \tag{24}$$

where f is the coefficient of rolling resistance.

The steering resistance torques M_{Rl} and M_{Rr} on both sides of the track can be expressed as follows:

$$\begin{cases} M_{Rl} = \int_{-\frac{L}{2}}^{\frac{L}{2}} (c + p_l \tan\phi)\left(1 - e^{-\frac{j_l}{K}}\right) b\sin(\psi_l + \pi)\, x\mathrm{d}x \\ M_{Rr} = \int_{-\frac{L}{2}}^{\frac{L}{2}} (c + p_r \tan\phi)\left(1 - e^{-\frac{j_r}{K}}\right) b\sin(\psi_r + \pi)\, x\mathrm{d}x. \end{cases} \tag{25}$$

The steering balance equation of the tracked vehicle can be expressed as follows:

$$\begin{cases} ma_x = F_{xr} + F_{xl} - F_{Rl} - F_{Rl} \\ ma_y = F_{yr} + F_{yl} \\ I_z\ddot{\theta} = \dfrac{B}{2}(F_{xl} - F_{xr}) - \dfrac{B}{2}(F_{Rl} - F_{Rr}) - M_{Rl} - M_{Rr}. \end{cases} \tag{26}$$

By combining Formulas (14) and (26), the accelerations $\dot{v}_x$, $\dot{v}_y$ and the yaw angular acceleration $\ddot{\theta}$ of the tracked vehicle in x-direction and y-direction can be expressed as follows:

$$\begin{cases} \dot{v}_x = (F_{xr} + F_{xl} - F_{Rl} - F_{Rr})/m - v_y\dot{\theta} \\ \dot{v}_y = (F_{yr} + F_{yl})/m + v_x\dot{\theta} \\ \ddot{\theta} = \left(\dfrac{B}{2}(F_{xl} - F_{xr}) - \dfrac{B}{2}(F_{Rl} - F_{Rr}) - M_{Rl} - M_{Rr}\right)/I_z. \end{cases} \tag{27}$$

The changes of the parameters of the tracked vehicle steering process were calculated, and the sand road was selected. The vehicle structure and road parameters are shown in Table 1.

When the tracked vehicle turned at different theoretical centroid speeds v_{th}, the relationship between $\dot{\theta}$ and Δu is shown in Fig. 5.

TABLE 1. Vehicle and road parameters.

Road parameters (sand road)			
$c(P_a)$	K(cm)	$\phi(^\circ)$	f
1.3	1.2	31.1	0.065
Vehicle parameters			
m(kg)	I_z(kg·m^2)	L(m)	B(m)
36500	13000	3.78	2.64
b(m)	l(m)	r(m)	h(m)
0.58	0.18	0.283	1.159
i_q	i_p	i_M	i_h
0.7	0.633	4	4.75
k	η	$\delta_{sw}(^\circ)$	i_{bn}
2.375	0.9	[−50,50]	6/2.8/2/1.43/0.91

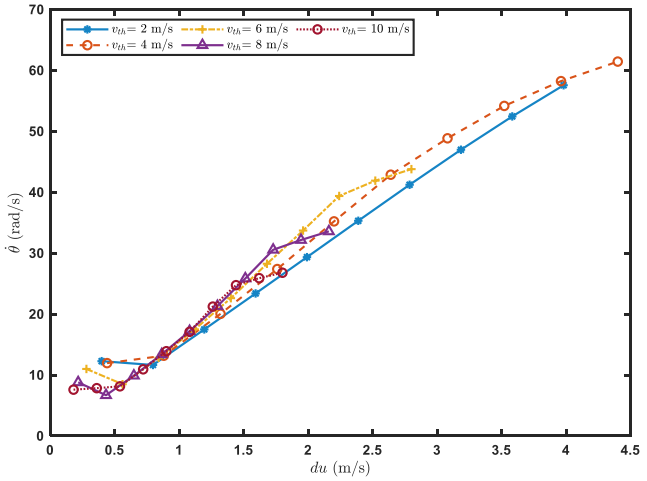

FIGURE 5. $\dot{\theta}$ **variations with** Δu **when the tracked vehicle turned on a sand road.**

IV. STEERING CONTROLLER DESIGN

A. COMPREHENSIVE EVALUATION INDEX

According to the comprehensive evaluation index J_{TE} of the tracked vehicle handling stability, the control effect of the designed SBW system controller was evaluated [23]. The selected evaluation indices mainly the following:

(1) The trajectory tracking evaluation index J_e, which is used to evaluate the accuracy of the tracked vehicle tracking reference trajectory, is expressed as follows:

$$\begin{cases} J_{e1} = \int_0^{t_n} \left(\dfrac{f(t) - y(t)}{\hat{E}} \right)^2 \mathrm{d}t \\ J_{e2} = \int_0^{t_n} \left(\dfrac{v\beta}{\hat{\beta}} \right)^2 \mathrm{d}t \\ J_e = \sqrt{\dfrac{w_{e1}J_{e1}^2 + w_{e2}J_{e2}^2}{w_{e1} + w_{e2}}}, \end{cases} \tag{28}$$

where t_n is the sampling time, $f(t)$ is the expected trajectory at time t, and $y(t)$ is the actual position of the vehicle at time t. $\hat{E}$ is the standard value of the trajectory tracking error, where $\hat{E} = 1$. $\dot{\beta}$ is the sideslip centroid angular velocity. $\hat{\beta}$ is the standard value of the sideslip centroid angular velocity, $\hat{\beta} = 0.8g$, g is the acceleration of gravity, where $g = 9.8\mathrm{m}^2/\mathrm{s}$. w_{e1} and w_{e2} are weights, where $w_{e1} = 0.8$ and $w_{e2} = 0.2$.

(2) The evaluation index of the handling burden J_b based on according to the change of the steering wheel angular velocity can be expressed as follows:

$$J_b = \int_0^{t_n} \left(\frac{\dot{\delta}_{sw}(t)}{\hat{\dot{\delta}}_{sw}} \right)^2 \mathrm{d}t, \tag{29}$$

where $\hat{\dot{\delta}}_{sw}$ is the standard value of the steering wheel angular velocity, $\hat{\dot{\delta}}_{sw} = 1\mathrm{rad/s}$.

(3) The evaluation index J_r of the tracked vehicle rollover risk is expressed as follows:

$$J_r = \int_0^{t_n} \left(\frac{a_y(t)}{\hat{a}_y} \right)^2 \mathrm{d}t, \tag{30}$$

where $\hat{\delta}_{sw}$ is the standard value of the lateral acceleration, and $\hat{\delta}_{sw} = 1\mathrm{rad/s}$.

(4) The evaluation index J_s of the side slip risk of the tracked vehicle is expressed as follows:

$$\begin{cases} J_{sl} = \left(\dfrac{F_{yl}(t)/(P_l(t)\,bL)}{\hat{\mu}} \right)^2 \\ J_{sr} = \left(\dfrac{F_{yr}(t)/(P_r(t)\,bL)}{\hat{\mu}} \right)^2 \\ J_s = \max(J_{sl}, J_{sr}), \end{cases} \tag{31}$$

where $\hat{\mu}$ is the standard value of the lateral adhesion coefficient, $\hat{\mu} = 0.3g$.

The comprehensive evaluation index of the tracked vehicle handling stability and comfort is the weighted average of the four evaluation indices, which is expressed as follows:

$$J_{TE} = \sqrt{\frac{w_e J_e^2 + w_b J_b^2 + w_r J_r^2 + w_s J_s^2}{w_e + w_b + w_r J_r^2 + w_s J_s^2}}, \tag{32}$$

where $w_e = w_b = w_r = w_s = 0.25$.

B. DESIGN OF STEERING CONTROLLER

The yaw rate gain K_r was selected as the control target, and the PSO algorithm was used to obtain the optimal K_r in real time, which was applied for the steering control of the tracked vehicle. The PSO algorithm has a strong global optimization capability, and the solution process is shown in Fig. 6, where i is the current number of iterations, N is the maximum number of iterations, and D is the particle swarm dimension.

The particle swarm velocity update equation of the i-th iteration is as follows:

$$\begin{aligned} v_{K_r}(i+1) = {} & w v_{K_r}(i) + c_1 r_1 \left(K_{rp}(i) - K_r(i) \right) \\ & + c_2 r_2 \left(K_{rg}(i) - K_r(i) \right), \end{aligned} \tag{33}$$

where w is the inertia weight, c_1 is the individual learning weight, c_2 is the group learning weight, and r_1 and r_2 are random numbers generated in the range of [0, 1].

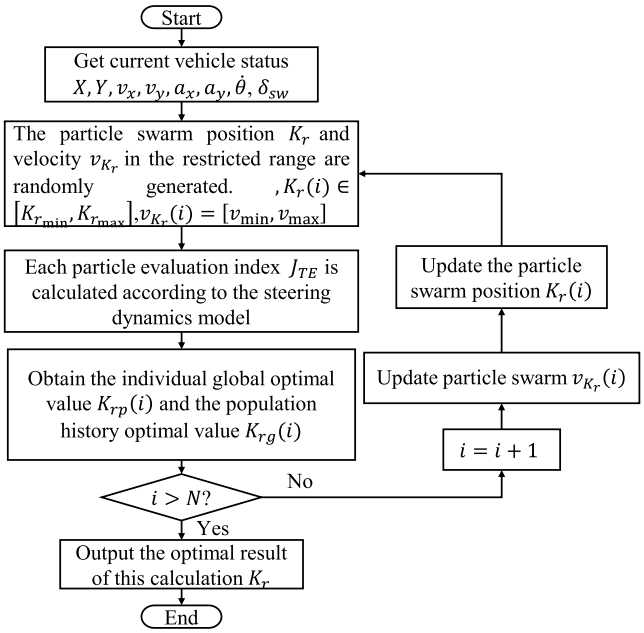

FIGURE 6. Steering controller solution process based on the particle swarm optimization (PSO) algorithm.

The particle swarm position update equation can be expressed as follows:

$$K_r(i+1) = K_r(i) + v_{K_r}(i+1) \tag{34}$$

The maximum number of iterations was set as the termination condition of the PSO controller optimization. When the number of iterations exceeded the maximum number of iterations, the historical optimal value of the output group was used as the control quantity of the yaw rate gain at this time.

The process of solving for the corresponding comprehensive evaluation index J_{TE_p} by substituting the position K_{r_p} of a single particle p into the tracked vehicle steering dynamics equation is shown in Fig. 7.

C. DRIVER MODEL

The driver model is an important tool for analyzing the performance of a human-vehicle closed-loop system. Based on the previous work of Guo et al. [24], a driver's ideal lateral acceleration preview model was established. For a known expected trajectory, the driver's ideal lateral acceleration preview model is shown in Fig. 8. XOY is the geodetic coordinate system, and x_rOy_r is the relative coordinate system. $X(t)$ and $Y(t)$ are the absolute coordinates of the centroid of the tracked vehicle at time t, $x_r(t)$ and $y_r(t)$ are the relative coordinates of the centroid of the tracked vehicle at time t, and θ is the yaw angle of the tracked vehicle.

The relationship between x_rOy_r and XOY can be expressed as follows:

$$\begin{cases} x_r = X\cos\theta + Y\sin\theta \\ y_r = Y\cos\theta - X\sin\theta \end{cases} \tag{35}$$

Assuming that θ is constant at time t, the velocity components of the centroid of the tracked vehicle in the X-direction and Y-direction can be expressed as follows:

$$\begin{cases} \dot{X} = v_{x_r}\cos\theta - v_{yr}\sin\theta \\ \dot{Y} = v_{xr}\sin\theta + v_{yr}\cos\theta \end{cases} \tag{36}$$

If the driver's preview time is T, the abscissa of the preview point in the geodetic coordinate system can be expressed as follows:

$$X(t+T) = X(t) + \dot{X}T. \tag{37}$$

$Y(t+T)$ can be obtained by the known expected trajectory function $f(t)$. The coordinate $y_r(t+T)$ transformed using Formula (35) can be expressed as follows:

$$y_r(t+T) = Y(t+T)\cos\theta - X(t+T)\sin\theta \tag{38}$$

According to the principle of the minimum expected trajectory error, the ideal lateral acceleration $\ddot{y}_r(t)^*$ can be determined as follows:

$$\ddot{y}_r(t)^* = \frac{2}{T^2}y(t+T) - y_r(t) - T\dot{y}(t). \tag{39}$$

According to the preview following theory, the steering wheel angle δ_{sw}^* can be obtained as follows:

$$\delta_{sw}^* = \ddot{y}(t)^* \frac{1+t_c s}{G_{ay}} \frac{e^{-t_d s}}{1+t_h s}, \tag{40}$$

where G_{ay} is the lateral acceleration gain, t_c is the steering derivative time constant, t_d is the driver's nervous system response delay time, t_h is the operation delay time considering the driver's arm operation and steering wheel inertia.

V. SIMULATION

The steering control simulation model of a zero-difference tracked vehicle was established by MATLAB/Simulink, and the proposed steering control method was simulated and verified. The driving model of the tracked vehicle was established according to the work of Purdy et al. [25]. The simulation model structure is shown in Fig. 9. Three methods were selected to control the steering of the tracked vehicle:

1) Method 1: steering control of the tracked vehicle with fixed i_ε, where $i_\varepsilon = 60$,

2) Method 2: fixed yaw rate gain control method, where $K_r = 0.6$,

3) Method 3: steering controller based on PSO algorithm.

The fixed yaw rate gain was set to $K_r = 0.6$, and the variations of i_ε are shown in Fig. 10.

A. SIMULATION EXPERIMENT OF CONTINUOUS STEERING OF TRACKED VEHICLE BASED ON SINUSOIDAL REFERENCE TRAJECTORY

1) LOW-SPEED STEERING CONTROL

The tracked vehicle was controlled by three methods to steer continuously according to the sinusoidal reference trajectory at $v_{th} = 3$ m/s in 2nd gear. Fig. 11 shows the steering trajectories. At low speed, all three methods could control the tracked

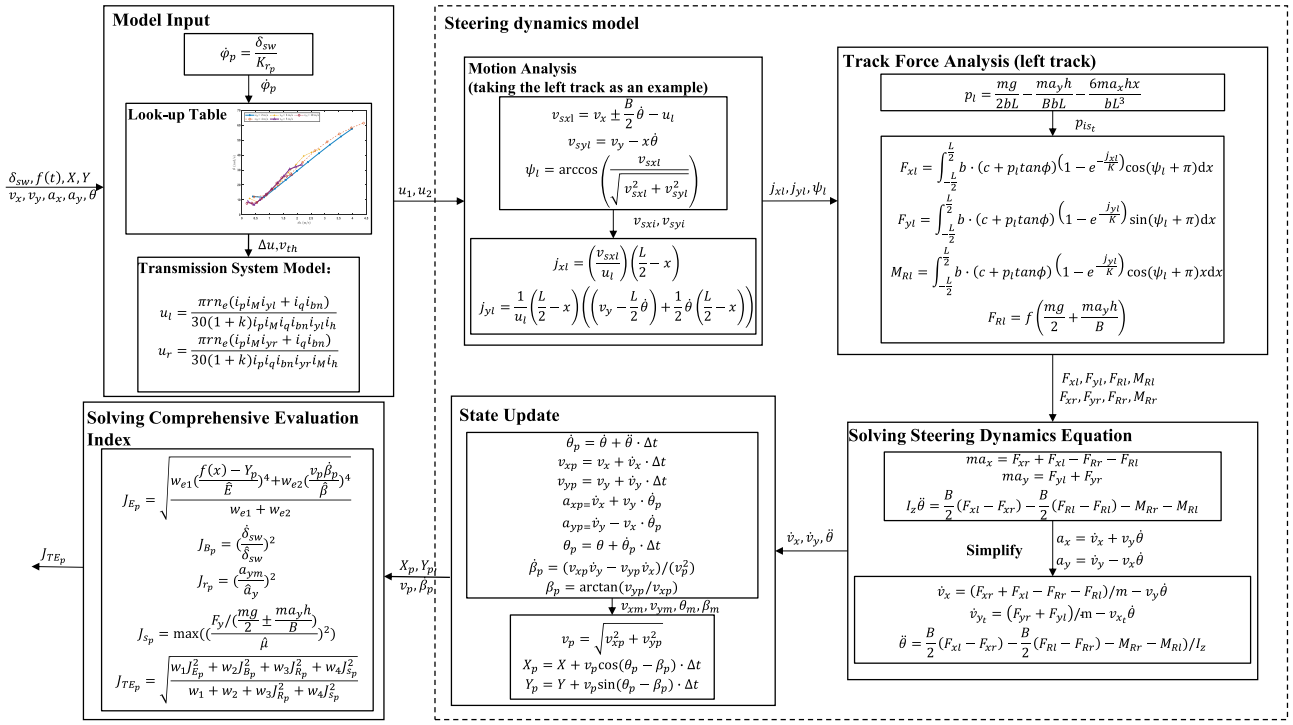

FIGURE 7. Solution process of single-particle comprehensive evaluation index.

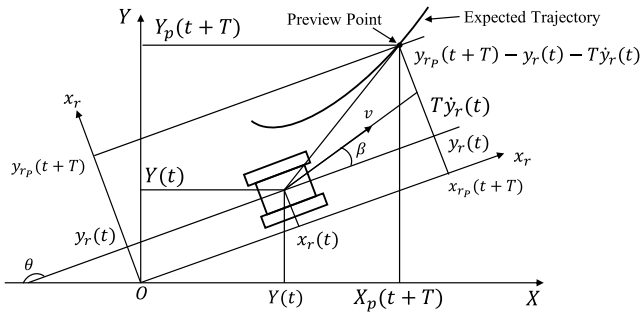

FIGURE 8. The driver's ideal lateral acceleration preview model.

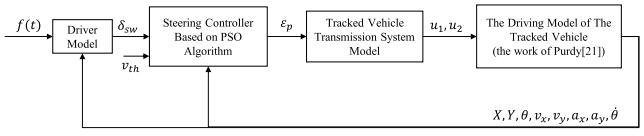

FIGURE 9. Simulation model structure.

TABLE 2. Parameters of drive model and steering controller.

Driver Model	
$T(s)$	1
$T_c(s)$	0.55
$t_d(s)$	0.3
$T_h(s)$	0.1
G_{ay}	2.5
Steering Controller	
D	10
N	30
w	0.5
c_1	0.5
c_2	0.5
$[K_{r\min}, K_{r\max}]$	$[0,1]$
$[v_{Kr\min}, v_{Kr\min}]$	$[-0.02,0.02]$

vehicle to follow the reference trajectory, with method 3 controlling the tracked vehicle with a higher trajectory tracking accuracy. Fig. 12 shows the variations of $\dot{\theta}$. When the tracked vehicle steering was controlled by method 1, $\dot{\theta}$ varied significantly, and $\dot{\theta}_{\max} = 0.3$ rad/s. The large variations of $\dot{\theta}$ reduced the steering stability of the tracked vehicle. Fig. 13 shows the change of the steering wheel angle. Under the control of method 1, the steering wheel variations of the tracked vehicle increased. The large change of the steering wheel angle made the driver's steering operation behavior cumbersome and increased the driver's driving burden. Under the control of methods 2 and 3, the steering wheel angle of the tracked vehicle changed less, and the steering wheel was more sensitive, which was more in line with the driver's driving habits when the tracked vehicle turned at low speed. Fig. 14 shows the change of comprehensive evaluation index. Under the control of method 3, the comprehensive evaluation index of the tracked vehicle was significantly lower than that of methods 1 and 2. The simulation results illustrated that the designed PSO-algorithm-based steering controller was

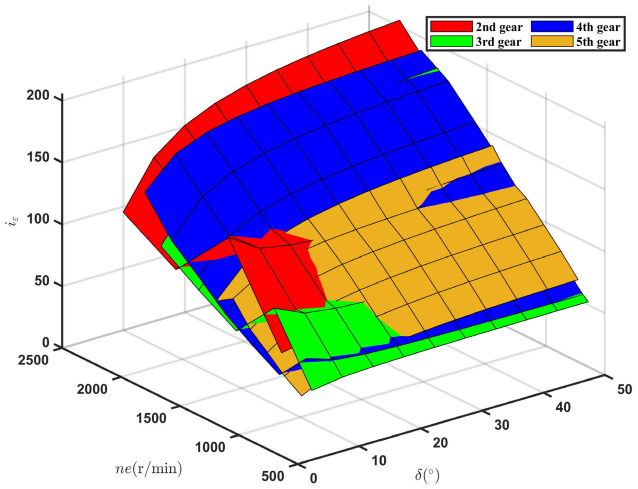

FIGURE 10. Variations of i_ε at $K_r = 0.6$.

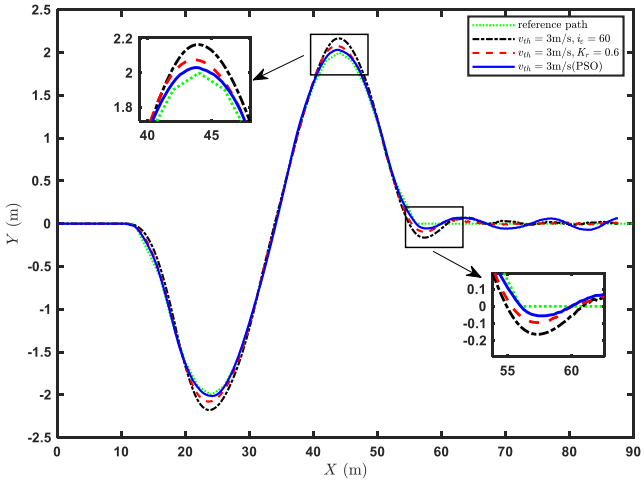

FIGURE 11. Driving trajectories when the tracked vehicle was continuously steered at $v_{th} = 3$ m/s.

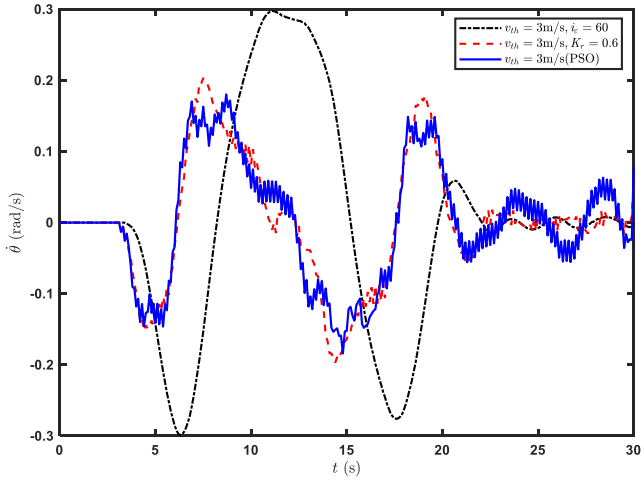

FIGURE 12. Variations of $\dot{\theta}$ when the tracked vehicle was continuously steered at $v_{th} = 3$ m/s.

more suitable for low-speed steering control of the tracked vehicle.

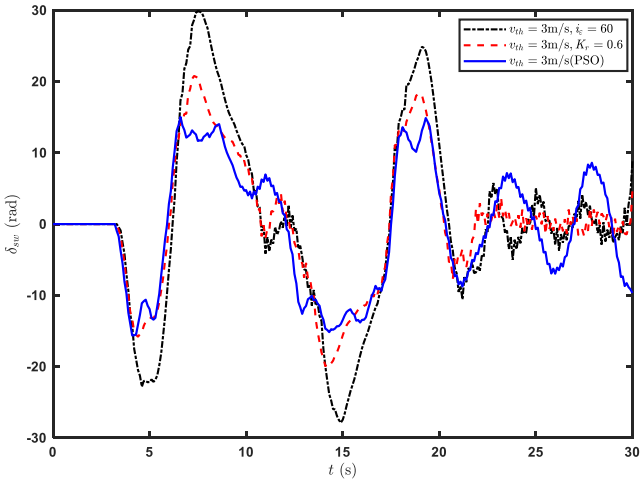

FIGURE 13. Variations of the steering wheel angle when the tracked vehicle was continuously steered at $v_{th} = 3$ m/s.

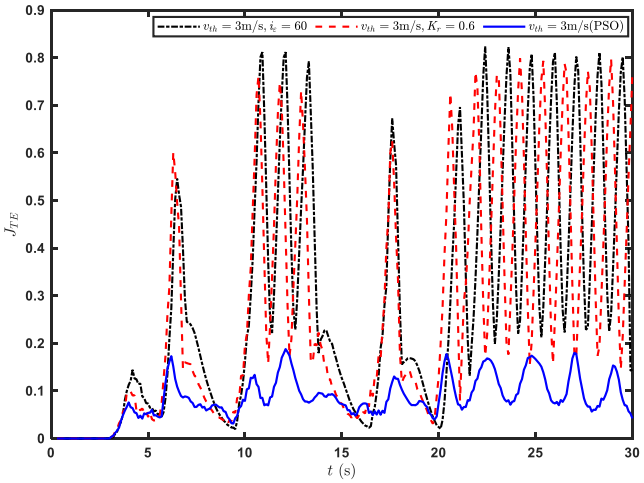

FIGURE 14. Variations of the comprehensive evaluation index when the tracked vehicle was continuously steered at $v_{th} = 3$ m/s.

2) HIGH-SPEED STEERING CONTROL

The tracked vehicle was controlled by three methods to steer continuously according to the sinusoidal reference trajectory at $v_{th} = 6$ m/s in 3rd gear. Fig. 15 shows the steering trajectories. Compared with the steering performance of the tracked vehicle at $v_{th} = 3$ m/s, method 1 had difficulty accurately controlling the tracked vehicle to track the expected trajectory at $v_{th} = 6$ m/s. The steering trajectory of the tracked vehicle oscillated around the reference trajectory. The reason was that the steering wheel was too sensitive at high speed. The driver's response and operation delay could not meet the driving requirements of the high-speed steering control of the tracked vehicle using method 1. In order to improve the steering stability, it was necessary to increase the i_ε of the tracked vehicle at high speed. Under the control of methods 2 and 3, the trajectory tracking error of the tracked vehicle increased compared with that at low speed. The variations of $\dot{\theta}$ are shown in Fig.16. When the tracked

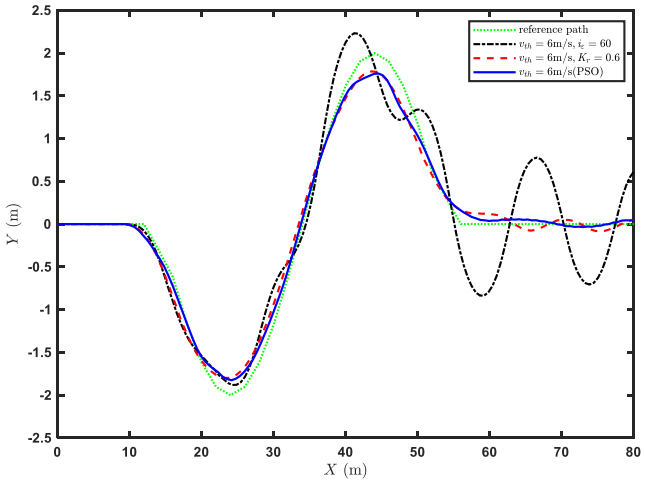

FIGURE 15. Driving trajectories when the tracked vehicle was continuously steered at v_{th} = 6 m/s.

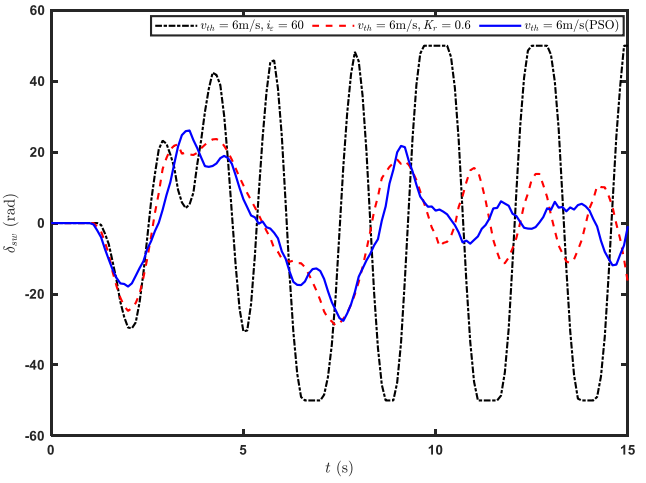

FIGURE 17. Variations of the steering wheel angle when the tracked vehicle was continuously steered at v_{th}= 6 m/s.

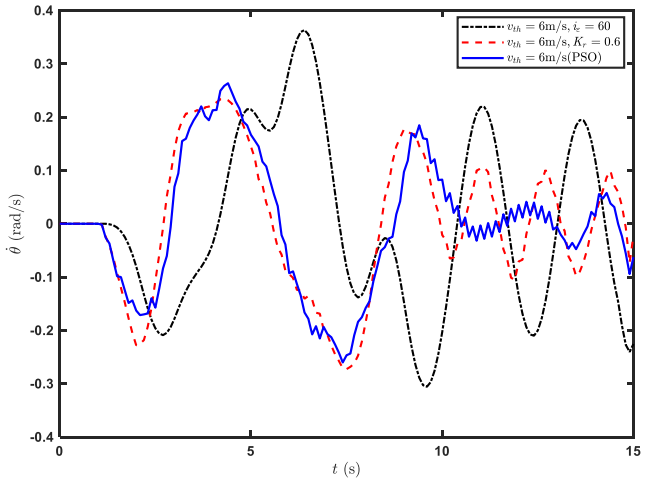

FIGURE 16. Variations of $\dot{\theta}$ when the tracked vehicle was continuously steered at v_{th} = 6 m/s.

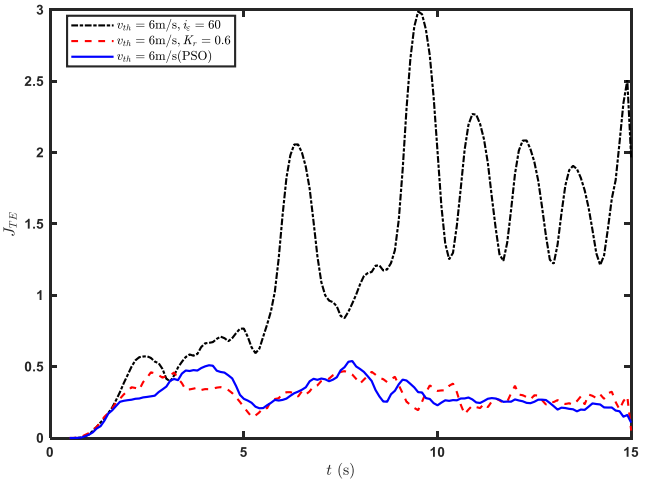

FIGURE 18. Variations of the comprehensive evaluation index when the tracked vehicle was continuously steered at v_{th}= 6 m/s.

vehicle steered at high speed, $\dot{\theta}$ increased and the steering stability of the tracked vehicle decreased. Fig. 17 shows the change of the steering wheel angle. Under the control of method 1, the steering wheel of the tracked vehicle continuously changed significantly. When the tracked vehicle turned at high speed, continuously and significantly adjusting the steering wheel angle would cause the tracked vehicle handling and steering stability to be low, and it would also greatly increase the driver's burden and improve the driving difficulty. For the driver, when using method 1 for vehicle steering control, in order to reduce the steering wheel variation range and increase the steering stability, the preview distance could be appropriately increased. Under the control of methods 2 and 3, the angular velocity of the steering wheel increased compared to that under the low-speed control of the tracked vehicle, the steering wheel sensitivity decreased, and the handling stability increased. The variations of the comprehensive evaluation index are shown in Fig. 18. When using methods 2 and 3 for tracked vehicle steering control, the comprehensive evaluation index was reduced, which showed that the two steering control methods had higher handling stability when the tracked vehicle was continuously steered at a higher speed according to the sinusoidal trajectory.

B. SIMULATION EXPERIMENT OF TRACKED VEHICLE STEERING BASED ON DOUBLE LANE CHANGE REFERENCE TRAJECTORY

1) LOW-SPEED STEERING CONTROL

The tracked vehicle steered according to the double lane change reference trajectory at v_{th} = 3 m/s in 2nd gear. Fig. 19 shows the variations of the steering trajectory. At low speed, the trajectory tracking accuracy of method 3 to control the tracked vehicle for a double lane change was higher. Fig. 20 shows the change of $\dot{\theta}$. When method 1 controlled the tracked vehicle steering, the yaw rate changed significantly, and the tracked vehicle steering stability was low.

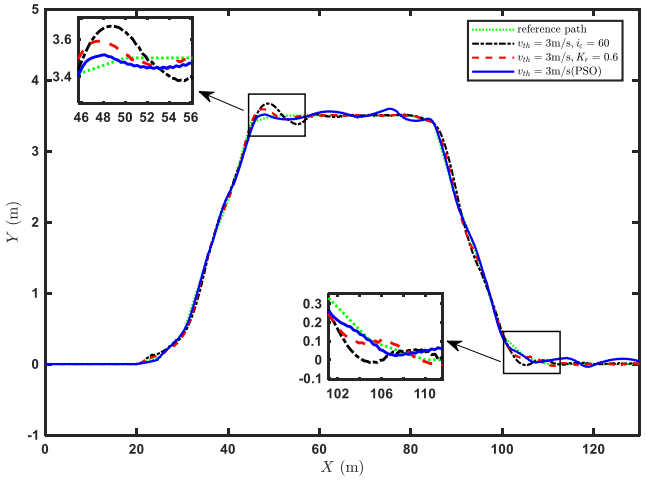

FIGURE 19. Steering trajectories when the tracked vehicle steered under double lane change conditions at $v_{th} = 3$ m/s.

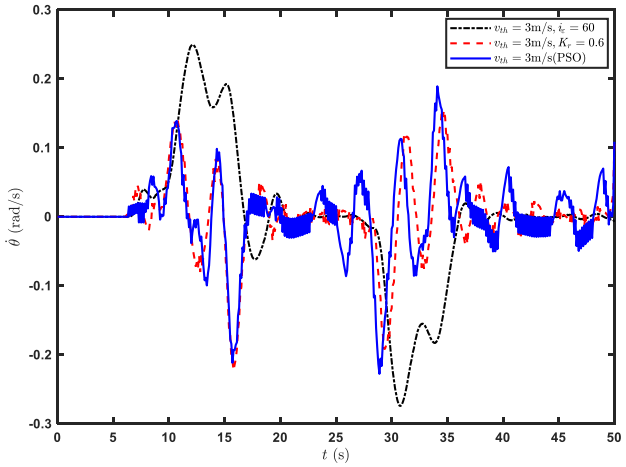

FIGURE 20. Variations of $\dot{\theta}$ when the tracked vehicle was steered under double lane change conditions at v_{th}= 3 m/s.

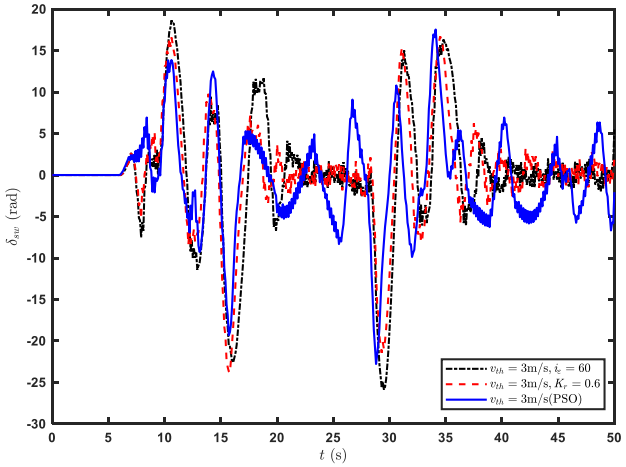

FIGURE 21. Variations of steering wheel angle when the tracked vehicle was steered under double lane change conditions at $v_{th} = 3$ m/s.

Fig. 21 shows the change of the steering wheel angle. The steering wheel variation range of method 3 was smaller than those in methods 1 and 2, which proved that method 3 was more sensitive for controlling the steering wheel of the tracked vehicle at low speed. Fig. 22 shows the change of the comprehensive evaluation index. At low speed, the handling stability of method 3 was better than that of methods 1 and 2 in controlling the steering of the tracked vehicle.

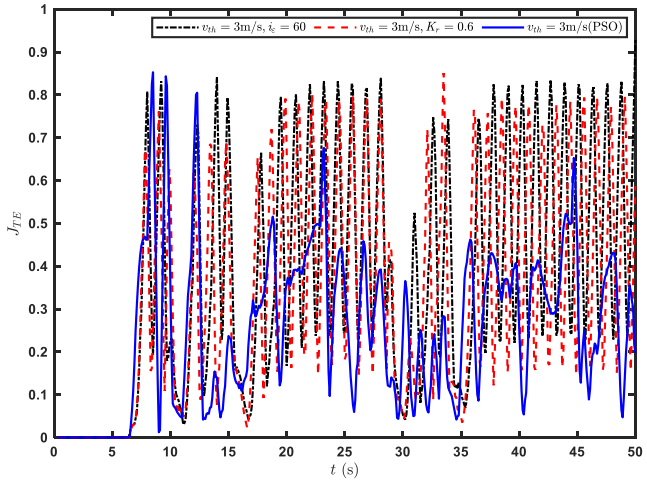

FIGURE 22. Variations of comprehensive evaluation index when the tracked vehicle was steered under double lane change conditions at $v_{th} = 3$ m/s.

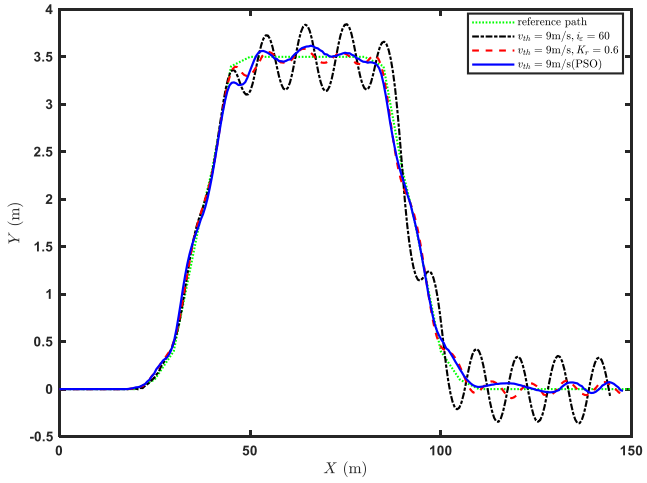

FIGURE 23. Steering trajectories when the tracked vehicle was steered under double lane change conditions at $v_{th} = 6$ m/s.

2) HIGH-SPEED STEERING CONTROL

The tracked vehicle steered according to the double lane change reference trajectory at $v_{th} = 6$ m/s in 3rd gear. Fig. 23 shows the steering trajectories. When using method 1 to control the tracked vehicle for the double lane change steering control, the tracked vehicle trajectory oscillated up and down around the reference trajectory. Fig. 24 shows the change of $\dot{\theta}$. The yaw rate of double lane change steering control increased and the steering stability decreased at high speed compared to those at the low speed. Fig. 25 shows the steering wheel

TABLE 3. Calculated values of the evaluation index of the steering control.

Path	Speed		$\bar{J}_e$	$J_{e_{max}}$	$\bar{J}_b$	$J_{b_{max}}$	$\bar{J}_r$	$J_{r_{max}}$	$\bar{J}_s$	$J_{s_{max}}$	$\bar{J}_{TE}$	$J_{TE_{\max}}$
Sinusoidal Reference Trajectory	v_{th} = 3 m/s	method 1	0.072	0.375	0.025	0.22	0.24	1.904	0.529	3.818	0.288	0.945
		method 2	0.054	0.266	0.019	0.147	0.24	1.893	0.537	3.827	0.268	0.95
		method 3	0.033	0.184	0.003	0.042	0.037	0.131	0.091	0.289	0.082	0.222
	v_{th} = 6 m/s	method 1	1.38	6.484	0.959	3.823	0.454	1.299	1.06	2.67	1.2	4.576
		method 2	0.118	0.591	0.04	0.222	0.172	0.871	0.389	2.652	0.289	0.893
		method 3	0.108	0.63	0.036	0.479	0.148	0.982	0.349	2.47	0.284	0.882
Double Lane Change	v_{th} = 3 m/s	method 1	0.046	0.31	0.028	0.25	0.34	1.847	0.753	3.843	0.371	0.944
		method 2	0.04	0.329	0.026	0.351	0.325	1.851	0.717	3.982	0.339	0.95
		method 3	0.025	0.236	0.014	0.162	0.17	1.561	0.38	3.426	0.253	0.926
	v_{th} = 6 m/s	method 1	0.376	4.069	0.28	3.001	0.207	1.439	0.477	2.85	0.306	2.934
		method 2	0.06	0.993	0.054	0.837	0.099	1.112	0.189	2.636	0.193	0.91
		method 3	0.04	0.747	0.029	0.585	0.076	1.09	0.151	2.523	0.113	0.881

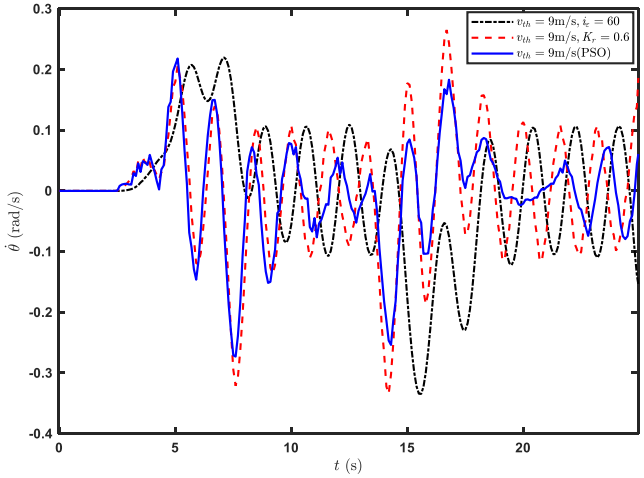

FIGURE 24. Variations of $\dot{\theta}$ when the tracked vehicle was steered under double lane change conditions at v_{th} = 6 m/s.

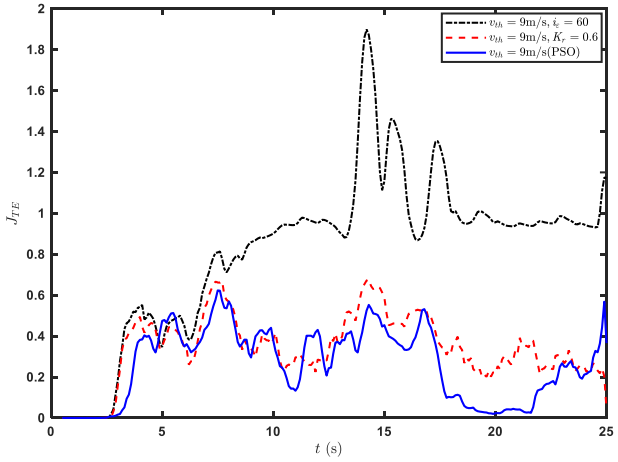

FIGURE 26. Variations of comprehensive evaluation index when the tracked vehicle was steered under double lane change conditions at v_{th} = 6 m/s.

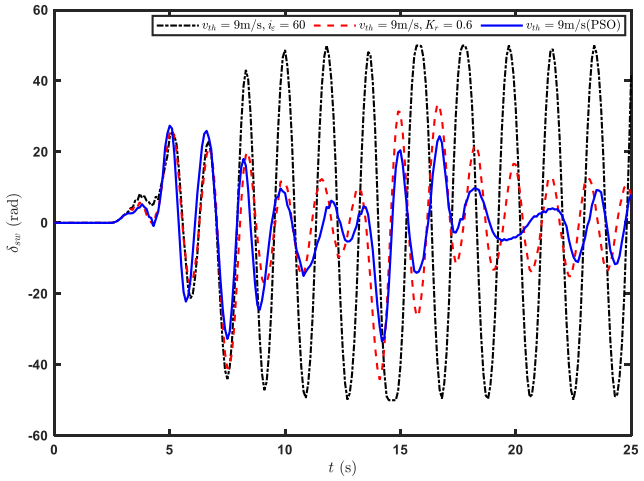

FIGURE 25. Variations of steering wheel angle when the tracked vehicle was steered under double lane change conditions at v_{th} = 6 m/s.

angle changes. When method 1 controlled the tracked vehicle steering, the steering wheel angle changed continuously and significantly, which could easily cause driver fatigue. Fig. 26 shows the change of the comprehensive evaluation index. When methods 2 and 3 were used to control the tracked vehicle steering in the double lane change condition at high speed, the tracked vehicle had better handling stability.

Table 3 shows the calculated values of the evaluation index of the steering control of the tracked vehicle at different speeds according to the sinusoidal reference trajectory and double lane change reference trajectory. From the calculation results of $\bar{J}_e$ and $J_{e_{\max}}$, when the tracked vehicle was controlled by method 1 for high-speed steering, the $\bar{J}_e$ and $J_{e_{\max}}$ values of the vehicle steering control increased rapidly, and the tracked vehicle had difficulty accurately following the reference trajectory. Methods 2 and 3 ensured the trajectory tracking accuracy of the tracked vehicle when steering at high speed. From the calculation results of $\bar{J}_b$ and $J_{b_{\max}}$, the $\bar{J}_b$ and $J_{b_{\max}}$ values when method 1 was used to control the vehicle steering at high speed significantly increased. The results showed that the driver had difficulty adapting to the steering wheel sensitivity of the tracked vehicle at high speed. In order to control the tracked vehicle to accurately track the reference trajectory, the steering wheel had to be adjusted continuously. In this case, experienced drivers with longer preview distances and shorter operation response times might be required to complete the corresponding steering operation. According to the calculation results of the rollover and skidding risk assessment indices $\bar{J}_r$, $\bar{J}_s$, $J_{r_{\max}}$

and $J_{s_{\max}}$ were still very large when using methods 2 and 3 to control the tracked vehicle for high-speed steering. The high-speed steering safety of the tracked vehicle was the next research focus. It can be seen from the calculation results of $\bar{J}_{TE}$ and $J_{TE_{\max}}$ that the control effect of method 2 was significantly improved compared with that of method 1 at high speed. However, the tracked vehicle handling stability when using method 2 to control vehicle steering was almost not improved at low speed. At low speed, the $\bar{J}_{TE}$ calculated by method 3 was reduced by 49.17% and 44.8% compared with those of methods 1 and 2, respectively. At high speed, the $\bar{J}_{TE}$ was reduced by 73.64% and 17.63%, respectively. The calculation results showed that compared with the other two methods, the steering controller based on the PSO algorithm could greatly improve the handling stability of the tracked vehicle and had better adaptability to changes of the steering conditions and vehicle speed.

VI. CONCLUSION

A conclusion might elaborate on the importance of the work or suggest applications and extensions. Aiming at the zero-differential steering control problem of the hydraulic-mechanical transmission tracked vehicle, a vehicle steering dynamics model was established based on the shear stress model, and a steer-by-wire controller was designed based on the PSO algorithm. The steering control simulation model of the tracked vehicle was established by using MATLAB/Simulink. The tracked vehicle was controlled by a method with a fixed i_ε, the fixed yaw rate gain control method, and an SBW controller designed using the PSO algorithm. The following conclusions could be drawn from the simulation results:

(1) When the tracked vehicle was steered at high speed with fixed i_ε, the steering wheel was too sensitive, making it difficult for the tracked vehicle to steer according to the reference trajectory. The continuous and significant change of the steering wheel angle increased the driver's burden, and the vehicle handling stability was poor.

(2) The fixed yaw rate gain method was used to control the steering of the tracked vehicle, which effectively improved the handling stability of the vehicle at high speed. However, compared with the fixed i_ε method, this method did not improve the vehicle handling stability at low speed.

(3) Compared with the fixed yaw rate gain control method, the vehicle steering controller based on the PSO algorithm further optimized the handling stability of the vehicle during high-speed steering. During low-speed steering, the vehicle handling stability was still significantly improved compared with that of the fixed i_ε method. This method has better control adaptability to the changes of the tracked vehicle speed and steering conditions.

ACKNOWLEDGMENT

The authors would like to thank LetPub (www.letpub.com) for its linguistic assistance during the preparation of this manuscript.

REFERENCES

[1] S. A. Mortazavizadeh, A. Ghaderi, M. Ebrahimi, and M. Hajian, "Recent developments in the vehicle Steer-by-Wire system," *IEEE Trans. Transport. Electrific.*, vol. 6, no. 3, pp. 1226–1235, Sep. 2020.

[2] W. Wang, X. Chen, and J. Wang, "Motor/generator applications in electrified vehicle chassis—A survey," *IEEE Trans. Transport. Electrific.*, vol. 5, no. 3, pp. 584–601, Sep. 2019.

[3] N. Guo, B. Lenzo, X. Zhang, Y. Zou, R. Zhai, and T. Zhang, "A real-time nonlinear model predictive controller for yaw motion optimization of distributed drive electric vehicles," *IEEE Trans. Veh. Technol.*, vol. 69, no. 5, pp. 4935–4946, May 2020.

[4] N. Guo, X. Zhang, Y. Zou, G. Du, C. Wang, and L. Guo, "Predictive energy management of plug-in hybrid electric vehicles by real-time optimization and data-driven calibration," *IEEE Trans. Veh. Technol.*, vol. 71, no. 6, pp. 5677–5691, Jun. 2022.

[5] G. Shi, "Influence of variable steering ratio for steer-by-wire system on vehicle handling stability," *Trans. Beijing Inst. Technol.*, vol. 28, no. 3, pp. 207–210, 2008.

[6] C. Wang, "Active front wheel steering control based on ideal transmission ratio," *Trans. Chin. Soc. Agricult. Eng.*, vol. 31, no. 4, pp. 85–90, 2015.

[7] Z. Cong, X. Jian, and M. N. Iqbal, "Review on automobile steering-by-wire system development," *Appl. Mech. Mater.*, vols. 130–134, pp. 2194–2197, Oct. 2011.

[8] G. Zhu, H. Yang, and F. Yu, "Controller design for an automobile steer-by-wire system," in *Proc. IEEE 28th Int. Symp. Ind. Electron. (ISIE)*, Jun. 2019, pp. 1492–1497.

[9] B. Schwarz and L. Eckstein, "Reduction of driving resistance by means of wheel-individual steer-by-wire systems," *ATZ Worldwide*, vol. 120, no. 1, pp. 44–49, Jan. 2018.

[10] L. Zhai, X. Zhang, Z. Wang, Y. M. Mok, R. Hou, and Y. Hou, "Steering stability control for four-motor distributed drive high-speed tracked vehicles," *IEEE Access*, vol. 8, pp. 94968–94983, 2020.

[11] Y. Deng, Y. Zhao, W. Pi, Y. Li, S. Feng, and Y. Du, "The influence of nonlinear stiffness of novel flexible road wheel on ride comfort of tracked vehicle traversing random uneven road," *IEEE Access*, vol. 7, pp. 165293–165302, 2019.

[12] Y. Zhang, "Research on characteristics of tracked vehicle steering on slope," *Math. Problems Eng.*, vol. 2021, pp. 1–18, Jan. 2021.

[13] Y. W. Chai, Y. Abe, Y. Kano, and W. Abe, "A study on adaptation of SBW parameters to individual driver's steer characteristics for improved driver-vehicle system performance," *Vehicle Syst. Dyn.*, vol. 44, no. 1, pp. 874–882, 2006.

[14] F. Li, L. Wang, C. Liao, and Y. Wu, "Active steering control strategy of steer-by-wire system based on variable steering ratio," in *Proc. IEEE Conf. Expo. Transp. Electrific. Asia–Pacific (ITEC Asia–Pacific)*, Aug. 2014, pp. 1–5.

[15] S.-W. Oh, H.-C. Chae, S.-C. Yun, and C.-S. Han, "The design of a controller for the steer-by-wire system," *JSME Int. J. Ser. C, Mech. Syst. Mach. Elements Manuf.*, vol. 47, no. 3, pp. 896–907, Sep. 2004.

[16] S. M. H. Fahami, H. Zamzuri, S. A. Mazlan, and M. A. Zakaria, "Modeling and simulation of vehicle steer by wire system," in *Proc. IEEE Symp. Humanities, Sci. Eng. Res.*, Jun. 2012, pp. 765–770.

[17] Z. H. E. N. G. Hongyu, L. I. Jun, and Z. O. N. G. Changfu, "Optimization design of vehicle yaw rate gain for steer-by-wire," *J. Jilin Univ. Eng. Technol. Ed.*, vol. 42, no. 1, pp. 7–12, 2012.

[18] S. Krishna, S. Narayanan, and S. D. Ashok, "Fuzzy logic based yaw stability control for active front steering of a vehicle," *J. Mech. Sci. Technol.*, vol. 28, no. 12, pp. 5169–5174, Dec. 2014.

[19] Z. Dongzr, "Asimulation studyonthesteeringcontrolofa4WISEVbasedon LQRvariabletransmissionratiocontrol," *Automot. Eng.*, vol. 39, no. 1, pp. 79–85, 2017.

[20] Z. Jin, W. Liang, and W. Zhao, "Multi-gains ratio of steer-by-wire system and anti-rollover control for vehicle," *Jixie Gongcheng Xuebao/J. Mech. Eng.*, vol. 56, no. 10, pp. 172–180, 2020.

[21] H. Wang, "Analyzing and testing verification the performance about high-speed tracked vehicles in steering process," *Chin. J. Mech.*, vol. 50, no. 16, pp. 162–172, 2014.

[22] R. Qiang, "Analysis and experiment of tracked vehicle steering torque based on shear stress model," *Acta ArmamentarII*, vol. 36, no. 6, p. 968, 2015.

[23] K. Guo, F. Ma, and F. Kong, "Driver model parameter identification of the driver-vehicle-road closed-loop system," *Automot. Eng.*, vol. 24, no. 1, pp. 20–24, 2002.

[24] K. Guo, "Progress of the human-vehicle closed-loop system manoeuvrability's evaluation and optimization," *Jixie Gongcheng Xuebao Chin. J. Mech. Eng. China*, vol. 39, no. 10, pp. 27–35, 2003.
[25] D. J. Purdy, D. Simner, D. Diskett, A. Duncan, P. J. H. Wormell, and C. Stonier, "An experimental and theoretical investigation into the roll-over of tracked vehicles," *Proc. Inst. Mech. Eng., D, J. Automobile Eng.*, vol. 230, no. 3, pp. 291–307, Feb. 2016.

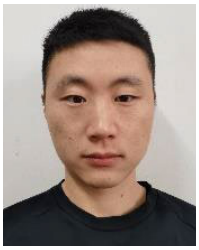

WEIJIAN JIA (Student Member, IEEE) received the M.S. degree in vehicle engineering from the Army Academy of Armored Forces, China, in 2020, where he is currently pursuing the Ph.D. degree with the Department of Vehicle Engineering. His main research interests include vehicle transmission systems and vehicle chassis control.

XIXIA LIU (Member, IEEE) is currently a Professor with the Department of Vehicle Engineering, Army Academy of Armored Forces, China. His main research interests include vehicle dynamics research, vehicle transmission system research, and unmanned system planning and control.

CHUANQING ZHANG (Member, IEEE) is currently an Associate Professor with the Department of Vehicle Engineering, Army Academy of Armored Forces, China. His main research interests include unmanned vehicle remote communication and robot control.

MIANHAO QIU (Member, IEEE) is currently an Associate Professor with the Department of Vehicle Engineering, Army Academy of Armored Forces, China. His main research interests unmanned system environment perception, decision planning, and system integration.

YONGYING TAN (Member, IEEE) received the Ph.D. degree from the Department of Vehicle Engineering, Army Academy of Armored Forces, Beijing, China, in 2020. He is currently an Engineer with the Beijing Special Engineering and Design Institute. His research interests include robotics and control.

ZHANG YU (Member, IEEE) received the B.S. degree in mechanical engineering from the Beijing Institute of Technology, China, in 2011, and the M.S. degree in mechanical engineering from the Army Academy of Armored Forces, China, in 2013, where he is currently pursuing the Ph.D. degree in mechanical engineering. He is a Lecturer with the Department of Vehicle Engineering, Army Academy of Armored Forces. His main research interests include unmanned system motion planning and environment perception.